

Article

Tuning Photophysical Properties of Donor/Acceptor Hybrid Thin-Film via Addition of SiO₂/TiO₂ Nanocomposites

Bandar Ali Al-Asbahi ^{1,2,*}, Mohammad Hafizuddin Hj. Jumali ³, M. S. AlSalhi ^{1,4}, Saif M. H. Qaid ^{1,5}, Amanullah Fatehmulla ¹, Wafa Musa Mujamammi ¹ and Hamid M. Ghaithan ¹

¹ Department of Physics & Astronomy, College of Sciences, King Saud University, Riyadh 11451, Saudi Arabia; malsalhi@ksu.edu.sa (M.S.A.); sqaid@ksu.edu.sa (S.M.H.Q.); aman@ksu.edu.sa (A.F.); walmujammi@ksu.edu.sa (W.M.M.); 436107632@student.ksu.edu.sa (H.M.G.)

² Department of Physics, Faculty of Science, Sana'a University, Sana'a 12544, Yemen

³ School of Applied Physics, Faculty of Science and Technology, Universiti Kebangsaan Malaysia, Selangor, Bangi 43600, Malaysia; hafizhj@ukm.edu.my

⁴ Research Chair in Laser Diagnosis of Cancers, College of Sciences, King Saud University, Riyadh 11451, Saudi Arabia

⁵ Department of Physics, Faculty of Science, Ibb University, Ibb 70270, Yemen

* Correspondence: balasbahi@ksu.edu.sa

Abstract: The influence of SiO₂/TiO₂ nanocomposites (STNCs) content on non-radiative energy transfer (Förster-type) from poly (9,9'-dioctylfluorene-2,7-diyl) (PFO) to poly [2-methoxy-5-(2-ethylhexyloxy)-1,4-phenylenevinylene] (MEH-PPV) using steady-state and time-resolved photoluminescence spectroscopies was investigated at room temperature. The improved energy transfer from PFO to MEH-PPV upon an increment of the STNCs was achieved by examining absorbance, emission (PL) and photoluminescence excitation (PLE) spectra. The shorter values of the quantum yield (ϕ_{DA}) and lifetime (τ_{DA}) of the PFO in the hybrid thin films compared with the pure PFO, indicating efficient energy transfer from PFO to MEH-PPV with the increment of STNCs in the hybrid. The energy transfer parameters can be tuned by increment of the STNCs in the hybrid of PFO/MEH-PPV. The Stern–Volmer value (k_{SV}), quenching rate value (k_q), Förster radius (R_0), distance between the molecules of PFO and MEH-PPV (R_{DA}), energy transfer lifetime (τ_{ET}), energy transfer rate (k_{ET}), total decay rate of the donor (TDR), critical concentration (A_0), and conjugation length (A_π) were calculated. The gradually increasing donor lifetime and decreasing acceptor lifetime, upon increasing the STNCs content, prove the increase in conjugation length and meanwhile enhance in the energy transfer.

Keywords: nanocomposite; donor/acceptor; optical properties; energy transfer; thin films



Citation: Al-Asbahi, B.A.; Hj. Jumali, M.H.; AlSalhi, M.S.; Qaid, S.M.H.; Fatehmulla, A.; Mujamammi, W.M.; Ghaithan, H.M. Tuning Photophysical Properties of Donor/Acceptor Hybrid Thin-Film via Addition of SiO₂/TiO₂ Nanocomposites. *Polymers* **2021**, *13*, 611. <https://doi.org/10.3390/polym13040611>

Academic Editor: Ana María Díez-Pascual

Received: 29 January 2021

Accepted: 15 February 2021

Published: 18 February 2021

Publisher's Note: MDPI stays neutral with regard to jurisdictional claims in published maps and institutional affiliations.



Copyright: © 2021 by the authors. Licensee MDPI, Basel, Switzerland. This article is an open access article distributed under the terms and conditions of the Creative Commons Attribution (CC BY) license (<https://creativecommons.org/licenses/by/4.0/>).

1. Introduction

The incorporation of inorganic nanostructures into the organic materials imparted interesting optoelectronic properties to nanocomposite materials and opened a new way for designing unique optical-based materials for optoelectronic applications. One of the most significant approaches to improve the efficiency of the optoelectronic devices, such as organic light emitting diodes (OLEDs), is through fabricated emissive layers based on donor/acceptor combinations [1–3]. The improvement of the optoelectronic properties and thus OLEDs emission efficiency can be achieved by controlling the donor/acceptor content and shifting the emission wavelength away from the donor absorption band by a non-radiative energy transfer from the donor excited state to that of the acceptor [4,5]. Despite the significant attention of such approach, intermolecular interaction can occur in the donor/acceptor combination and thus quench the device luminescence [6]. The incorporation of inorganic nanostructures into the donor/acceptor hybrid was successfully employed to overcome such problem and thus improved the device performance [2,7,8].

Recently, it was found that the incorporation of SiO₂/TiO₂ nanocomposites (STNCs) into the conjugated polymers plays a crucial role in improvement of OLED devices performance, where the STNCs possess the features of both SiO₂ and TiO₂ NPs [9,10].

Numerous approaches, such as solution blending method [2], sol–gel [11], in situ polymerization [12], and star-like polymer as nanoreactors [13], have been established to prepare well-defined organic/inorganic nanocomposites. In the recent studies, the effect of fixed ratio of individual TiO₂ or SiO₂ NPs and fixed STNCs on the energy transfer of the various blend ratios of poly [2-methoxy-5-(2-ethyl-hexyloxy)-1,4-phenylenevinylene] (MEH-PPV) and poly (9,9'-di-n-octylfluorenyl-2,7-diyl) (PFO) was investigated in details [7]. The ultraviolet and visible emission intensities of STNCs were greater than that of pristine TiO₂ or SiO₂ NPs, subsequently, the addition of the STNCs into the hybrids of the donor/acceptor enhanced the energy transfer properties [14].

Despite several reports representing the effect of incorporation TiO₂ or SiO₂ NPs on the physical properties of Donor/acceptor hybrid, there have been no reports on the effect of STNCs content on the tuning photophysical properties of PFO/MEH-PPV. In the current work, MEH-PPV (as acceptor) and PFO (as donor) were blended at fixed ratio and the tuning optical properties and the energy transfer parameters by various weight ratios of the STNCs will be demonstrated here in terms of quantum yield (φ_{DA}), lifetime (τ_{DA}), Stern–Volmer value (k_{SV}), quenching rate value (k_q), Förster radius (R_0), distance between the molecules of donor and acceptor (R_{DA}), energy transfer lifetime (τ_{ET}), energy transfer rate (k_{ET}), the total decay rate of the donor (TDR), the critical acceptor concentration (A_0), the conjugation length (A_π), and lifetime decay for the emission regions of donor and acceptor.

2. Materials and Methods

PFO and MEH-PPV with weight-average molecular weight 58,200 and 40,000 g/mol, respectively were purchased from Sigma Aldrich (Saint Louis, Missouri, USA) and were used as received without further purification. The SiO₂ NPs in amorphous phase was synthesized by sol-gel method, as reported in our previous study [15], and mixed with anatase TiO₂ NPs (which was purchased from Sigma Aldrich) to form SiO₂/20 wt% TiO₂ NCs (STNCs) as prepared in our previous report [14]. The fixed ratio of PFO/10 wt% MEH-PPV hybrid, in a toluene solvent produced by Fluka, was prepared with various weight ratios of STNCs: 5, 10, 15, and 20 wt% by solution blending method. A spin coating technique with 2000 rpm for 20 s was used to deposit 70 μ L from each sample onto a glass substrate (1.2 cm \times 2 cm). All samples were annealed at 120 °C in a vacuum oven to remove the solvent.

To collect the both absorption and emission spectra as well as lifetime decays, Perkin Elmer Lambda 900 ultraviolet–visible Spectrometer and an Edinburgh Instrument FLSP920 spectrophotometer were used respectively. The thin films morphology was characterized by field emission scanning electron microscope (FE-SEM) (Zeiss Supra 55VP, Oberkochen, Germany).

3. Results

3.1. Optical Properties

The normalized absorbance and emission spectra of pristine PFO and pristine MEH-PPV are shown in Figure 1. One absorbance peak at 397 nm corresponding to $\pi \rightarrow \pi^*$ transition appeared for PFO besides two emission peaks at 437 nm and 458 nm referring to 0 \rightarrow 0 and 0 \rightarrow 1 transition respectively, and a shoulder at 488 nm referring to 0 \rightarrow 2 transition. On the other side, two absorbance peaks at 339 nm and 508 nm appeared for MEH-PPV corresponding to 0 \rightarrow 1 and 0 \rightarrow 0 transition respectively, and two emission peaks at 600 nm and 637 nm referring to 0 \rightarrow 0 and 0 \rightarrow 1 transition respectively.

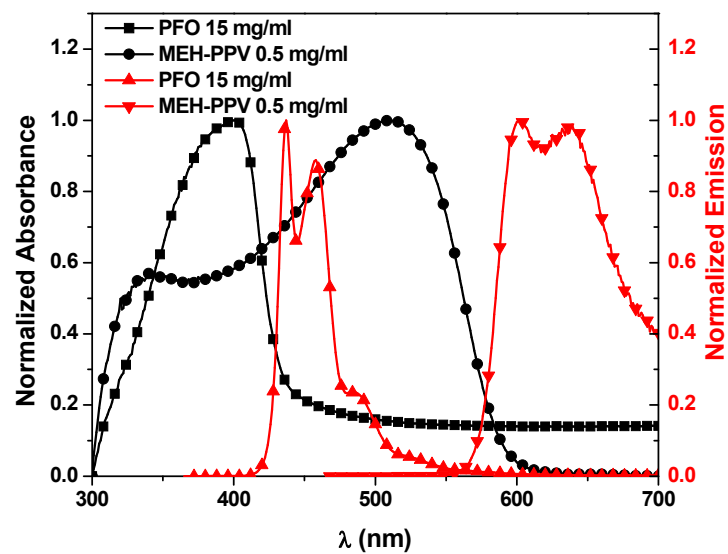


Figure 1. Normalized absorbance (black color) and emission spectra (red color) of PFO and MEH-PPV thin films.

The influence of the STNCs content on the absorbance of the donor/acceptor hybrid thin films is displayed in Figure 2. Two absorbance peaks at 394 nm and 512 nm can be observed referring to that of PFO and MEH-PPV respectively. It can be noticed that comparing with pristine conjugated polymers shown in Figure 1, the first peak (394 nm) was blue shifted ~ 3 nm whereas the second (512 nm) red shifted ~ 4 nm without appearing any new peaks, indicating no chemical interaction occurs [16]. Upon increment of STNCs into the PFO/10 wt% MEH-PPV hybrid, the absorbance of the first peak enhanced and blue shifted up to 14 nm, whereas the second peak improved and dramatically red shifted up to ~ 33 nm. Opposite trend was observed for the first peak with high content of the STNCs (>15 wt%) and new peak at ~ 310 nm referring to $0 \rightarrow 1$ transition of pure MEH-PPV with blue shift by ~ 29 nm. This means that the incorporation content of the STNCs in the hybrid is limited to improve both of the absorbance peaks related to both PFO and MEH-PPV. Moreover, the increasing absorbance with slightly blue shifting of the first peak that related to PFO is a strong indication that the STNCs have an effect on the conjugation length of the PFO [17] which will be corroborated later in Section 3.2.4.

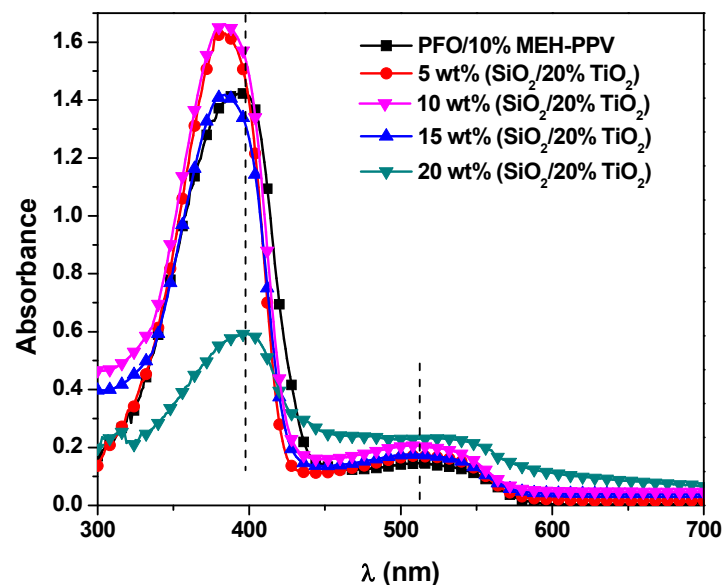


Figure 2. Absorbance spectra of PFO/MEH-PPV hybrid thin films with various ratios of STNCs.

Figure 3 shows emission spectra of PFO/MEH-PPV hybrid thin films with various ratios of STNCs photoexcited by 355 nm. Upon the inclusion of STNCs into the hybrids, a significant improvement in emission intensity from both PFO and MEH-PPV was detected. The MEH-PPV exhibited much faster intensity enhancement compared to PFO. It is reasonable to deduce that the significant enhanced emission intensity (Figure 3) and weak absorption of MEH-PPV in the hybrid thin films (Figure 2) is mainly due to improved energy transfer from PFO to MEH-PPV with increment the STNCs. In conjunction with the gradual enhancement of the three emission peaks that related to the PFO upon increment the STNCs, the emission peak of the MEH-PPV referring to the 0-0 transition was enhanced with fixed intensity even the content of the STNCs increased, whereas that peak for 0-1 transition was dramatically improved. As found in recent report [14], the STNCs with ratio of STNCs exhibited emission in the region 350–525 nm. Consequently, the enhancement in the emission intensity at region 400–525 nm referring to PFO in the PFO/MEH-PPV hybrids with the STNCs, resulted from the radiative transitions and oxygen vacancies that comes from the STNCs. Oxygen vacancies can act as an electron trap, resulting in enhancing the emission properties of the hybrid thin films by improving the UV light absorption. As a result, this enhancement leads to improve the emission intensity that is related to MEH-PPV through energy transfer mechanism from the PFO to MEH-PPV. Moreover, many studies proposed that the emission improvement in inorganic/conjugated polymers nanocomposites is mainly attributable to the formation of more extended chains and then increase the polymer conjugation length in addition to charge trapping effect [18–21]. On the other hand, the enhancing emission may result from the agglomeration of STNCs on the surface of the PFO/MEH-PPV hybrid, as seen in FE-SEM images (Figure 4).

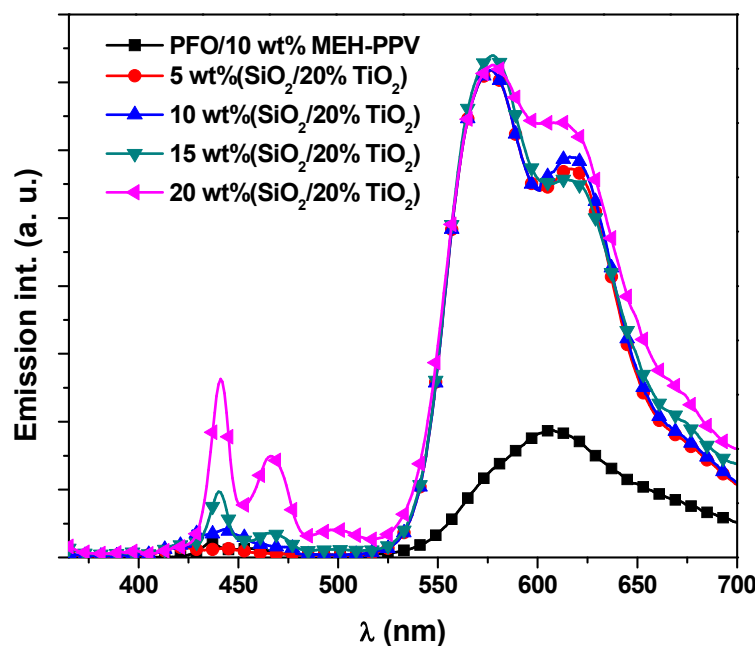


Figure 3. Emission spectra of PFO/MEH-PPV hybrid thin films with various ratios of STNCs.

The improved energy transfer from PFO to MEH-PPV upon increment the STNCs can be achieved by examining photoluminescence excitation (PLE) spectra. Figure 5 displays the PLE results acquired from the pristine PFO, pristine MEH-PPV, and PFO/10 wt% MEH-PPV hybrid with different STNCs contents collected at the monitoring emission wavelength of 550 nm. The very low PLE intensity of the PFO under the excitation wavelength (355 nm) and the very weak emission intensity at 550 nm in the emission spectrum of the PFO (see Figure 1), indicating that the emission at 550 nm mainly causes from MEH-PPV in the PFO/MEH-PPV hybrid. The PLE intensity peak at 355 nm increases obviously upon increment the STNCs content which is consistent with the emission intensity from

MEH-PPV shown in the emission spectra of the PFO/MEH-PPV with increasing the STNCs content. These results indicate that both photo-excitation in PFO and the content of STNCs contribute to the emission from MEH-PPV in the hybrid thin films. As the PFO/MEH-PPV hybrid with various content of STNCs are photo-excited by the 355 nm, the intrachain excimers can be formed in PFO during their lifetimes in addition to the charge trapping effect. Consequently, simultaneous enhanced emission from MEH-PPV and PFO is observed and then energy transfer from PFO to MEH-PPV improved.

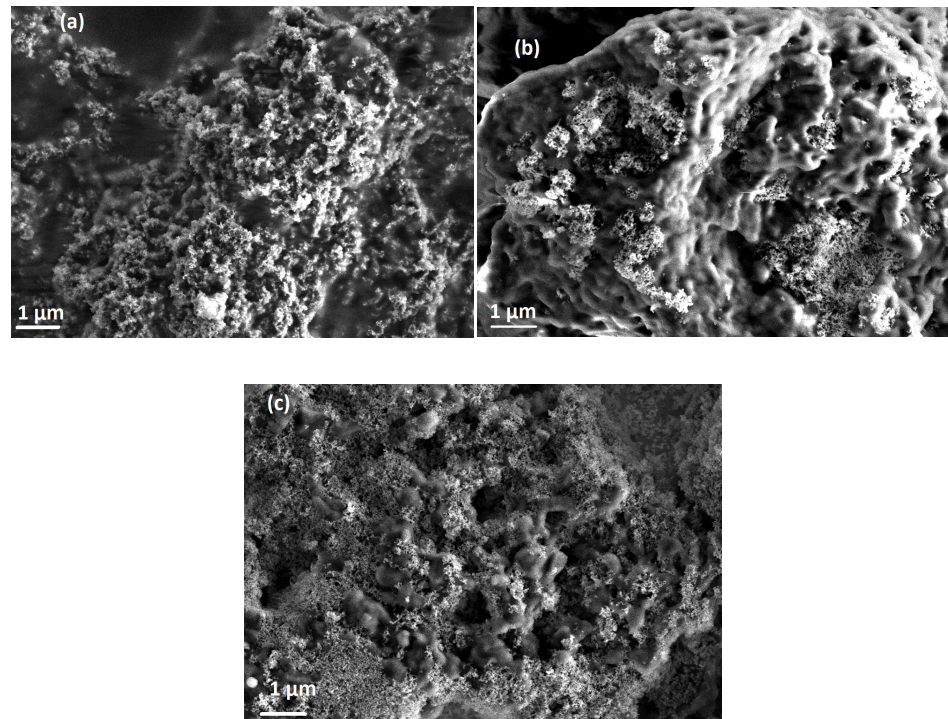


Figure 4. FE-SEM images of PFO/10 wt% MEH-PPV hybrid thin film with: (a) 10 wt% STNCs, (b) 15 wt% STNCs, and (c) 20 wt% STNCs.

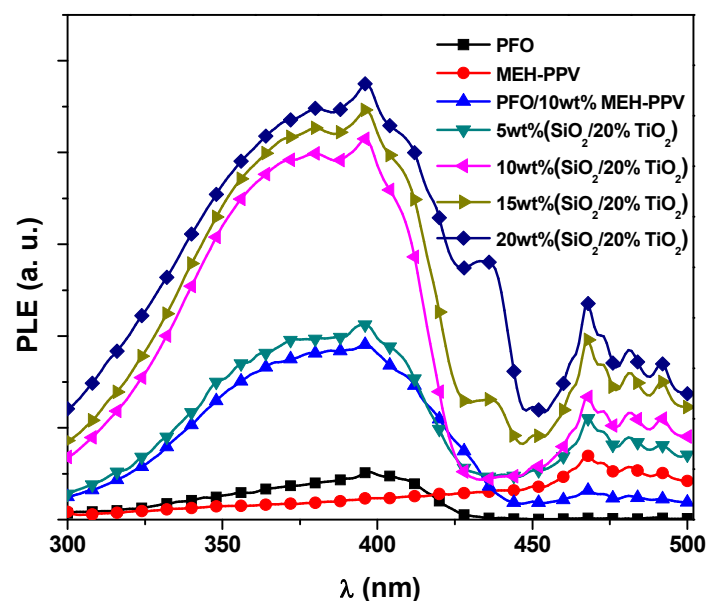


Figure 5. PLE spectra of the PFO, MEH-PPV, and PFO/MEH-PPV with various ratios of STNCs collected at the monitoring emission wavelength of 550 nm.

3.2. Energy Transfer Parameters

As found in recent report [7] at ratio of 10 wt% MEH-PPV in the hybrid thin film of PFO/MEH-PPV, the donor emission was quenched and the emission intensity of the acceptor concurrently reduced instead of increasing. This observation suggested that the energy transfer from the PFO to the significant number of MEH-PPV molecules was converted into heat, where these molecules acted as dark quenchers without any fluorescence. In the current work, a remarkable improvement in emission intensity from both PFO and MEH-PPV was verified with the inclusion of STNCs into the hybrid of PFO/10 wt% MEH-PPV (Figure 3). The MEH-PPV displayed much higher intensity improvement compared to PFO, conforming the improved energy transfer in present the STNCs.

The energy transfer parameters for the PFO/MEH-PPV hybrid with the STNCs was obtained at excitation wavelength of 355 nm which direct MEH-PPV excitation was insignificant and energy transfer from the PFO to the MEH-PPV occurred. In the sections below, numerous parameters were estimated to describe the influence of the STNCs on the energy transfer mechanism.

3.2.1. Quantum Yield and Lifetime of the Donor in the Hybrids

The tunable quantum yield (φ_{DA}) and lifetime (τ_{DA}) values of the PFO in the hybrid thin films was achieved by the addition of STNCs using the following formula [22]:

$$\frac{I_D}{I_{DA}} = \frac{\tau_D}{\tau_{DA}} = \frac{\varphi_D}{\varphi_{DA}} \quad (1)$$

where I_D and I_{DA} sign to the emission intensities of donor in the absence and presence of both quenchers (STNCs and acceptor), respectively.

The φ_{DA} was varied from 0.0137 to 0.2650 whereas the τ_{DA} from 6.57 ps to 127 ps with the increment of STNCs as tabulated in Table 1. However, these values of φ_{DA} and τ_{DA} still shorter than that of pure PFO thin film ($\varphi_D = 0.72$ and $\tau_D = 346$ ps) [1], indicating the efficient energy transfer from PFO to MEH-PPV upon increment the STNCs in the hybrid.

Table 1. Optical properties of PFO/10 wt% MEH-PPV hybrid thin film with various content of STNCs.

STNCs (wt%)	φ_{DA}	τ_{DA} (ps)	k_{nr} (ns) ⁻¹	k_{sv} (μM) ⁻¹	$k_q \times 10^{15}$ (M.S) ⁻¹	A_{π} (Å)	A_0 (mM)	$A_{1/2}$ (μM)
0	0.0137	6.57	150.1	1.24	3.57	-4.278	5.4	0.81
5	0.0389	18.7	51.4	0.420	1.21	-3.207	3.7	2.38
10	0.0814	39.1	23.5	0.188	0.543	-2.424	2.9	5.32
15	0.0907	43.6	20.9	0.166	0.480	-2.305	1.8	6.02
20	0.2650	127	5.8	0.041	0.119	-1.020	1.0	24.3

3.2.2. Stern–Volmer (k_{SV}) and Quenching Rate (k_q) Constants

The Stern–Volmer value (k_{SV}) of the donor/acceptor hybrid was moderated with addition of the STNCs using the following formula [23]:

$$\frac{I_D}{I_{DA}} = 1 + k_{SV}[A] \quad (2)$$

where $[A]$ is the acceptor concentration.

The values of k_{SV} dramatically decreased from 1.24 to 0.041 (μM)⁻¹ as summarized in Table 1. These values implied that 50% of the emission was quenched for the acceptor concentration ($A_{1/2}$) increases systematically from approximately 0.81 to 24.3 μM with increasing the STNCs (Table 1).

The quenching rate value ($k_q = \frac{k_{SV}}{\tau_D}$) was tuned by the incorporation of STNCs into the PFO/MEH-PPV hybrid, from 3.57×10^{15} to 0.119×10^{15} M⁻¹.S⁻¹ (Table 1). Since the minimum value for efficient quenching is 1×10^{10} M⁻¹.S⁻¹ [22], the high values of k_q in the current work indicate the STNCs well mixing with the PFO/MEH-PPV hybrid.

3.2.3. Förster Radius, Energy Transfer Rate, and Energy Transfer Lifetime

The integral values under the curves in Figure 6 were employed to calculate the critical distance of the energy transfer, R_0 (Förster radius) using the following equation:

$$R_0^6 = \frac{5.89 \times 10^{-5} \phi_D}{n^4} J(\lambda) \quad (3)$$

where n is the solvent refractive index [22,24]. The values of both $J(\lambda) = \int F(\lambda) \varepsilon_A(\lambda) \lambda^4 d\lambda$ and R_0 are presented in Table 2. With the addition of STNCs, the value of the $J(\lambda)$ significantly increased from 0.82×10^{15} to $21.8 \times 10^{15} \text{ M}^{-1} \cdot \text{cm}^{-1} \cdot \text{nm}^4$ and thus the R_0 tuned from 43.7 to 75.6 Å, which still in the range of 10–100 Å that confirm the efficient long-range dipole-dipole energy transfer (Förster type) upon increment the STNCs in the hybrid thin film [25,26].

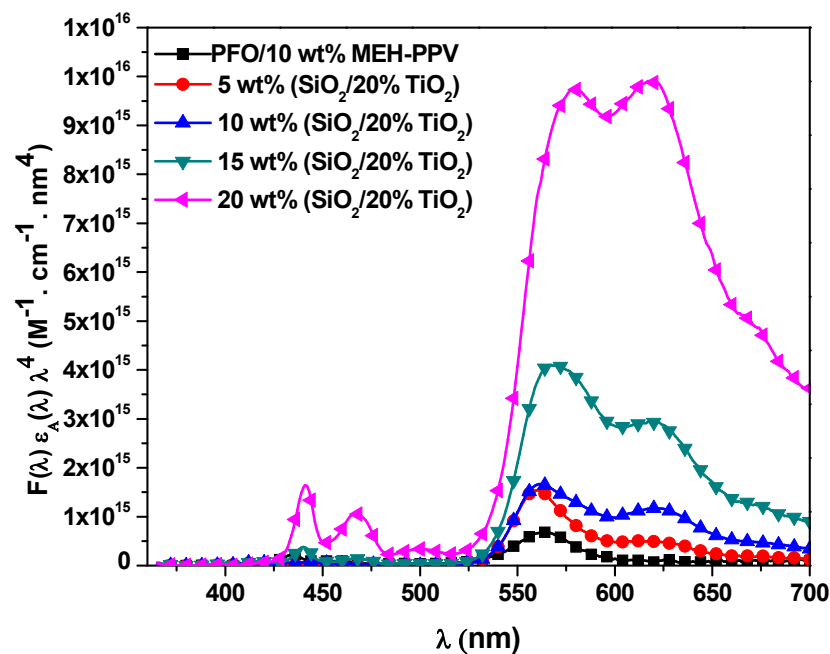


Figure 6. $F(\lambda) \varepsilon(\lambda) \lambda^4$ versus wavelength for PFO/MEH-PPV with various ratios of STNCs.

Table 2. Energy Transfer Parameters of PFO/10 wt% MEH-PPV hybrid thin film with various content of STNCs.

STNCs (wt%)	$J(\lambda) \times 10^{15} (\text{M}^{-1} \cdot \text{cm}^{-1} \cdot \text{nm}^4)$	R_0 (Å)	R_{DA} (Å)	$k_{ET} (\text{ns})^{-1}$	τ_{ET} (ps)	TDR (ns) ⁻¹
0	0.82	43.7	22.6	149	6.70	152
5	1.68	49.3	30.6	50.6	19.7	53.5
10	2.82	53.7	38.1	22.6	44.1	25.6
15	7.18	62.8	45.5	20.1	49.9	22.9
20	21.8	75.6	69.0	4.96	201	7.85

The distance between the molecules of PFO and MEH-PPV (R_{DA}) was calculated based on the Förster radius and emission intensities of the donor in absence and presence the acceptor using the following equation [27]:

$$1 - \frac{I_{DA}}{I_D} = \frac{R_0^6}{R_{DA}^6 + R_0^6} \quad (4)$$

As presented in Table 2, when the STNCs content increased from 0 to 20 wt%, the R_{DA} increased from 22.6 to 69.0 Å.

Additional evidence for the efficient incorporation of the STNCs on the energy transfer in the hybrid PFO/MEH-PPV can be found from the tunable values of energy transfer lifetime (τ_{ET}), total decay rate of the donor (TDR = $k_{ET} + \tau_D^{-1}$), and energy transfer rate (k_{ET}), which are calculated using the following expressions [22] and listed in Table 2.

$$\tau_{ET} = \frac{1}{[A]k_q} \quad \& \quad k_{ET} = \frac{1}{\tau_D} \left(\frac{R_0}{R_{DA}} \right)^6 \quad (5)$$

The τ_{ET} increased while the k_{ET} and TDR reduced with increment the STNCs into the donor/acceptor hybrid. This finding can be attributed to the increase in the distance between PFO (donor) and MEH-PPV molecules (acceptor) [28].

3.2.4. Critical Concentration of Acceptor (A_0) and Conjugated Length (A_π)

The concentration of the MEH-PPV should be lower than the critical concentration ($A_0 = \frac{447}{R_0^3}$), which is the concentration of the acceptor with 76% energy transfer [22], to suppress the intermolecular transfer in the PFO. The A_0 values of MEH-PPV can be significantly tuned by incorporation the STNCs. As presented in Table 1, it was varied from 5.4 to 1.0 mM with increasing the STNCs content.

The distance between the dipoles arising from the ground state (S_0) to the excited singlet state (S_1) transition is defined as the conjugation length (A_π) in the excited singlet state. It can be derived from the nonradiative rate constant (k_{nr}) and radiative rate constant (k_r) according to the following formula [29]:

$$A_\pi = \ln \left(\frac{k_r}{k_{nr}} \right) \quad (6)$$

Upon increment of the STNCs, the value of k_r exhibits approximately no change (2.08 ns^{-1}) while significant modification in the value of k_{nr} was observed, as listed in Table 1, indicating dominant non-radiative energy transfer and negligence radiative energy transfer. Therefore, A_π slightly increased with the increment of the STNCs. The increase in both values of R_{DA} and A_π with increment the STNCs showed that the STNCs increased the distance between the molecules of PFO and MEH-PPV.

The exponential increasing in ϕ_{DA} with A_π upon increment of the STNCs, as shown in Figure 7, demonstrate unique nanocomposites with high fluorescence as confirmed previously in Figure 3.

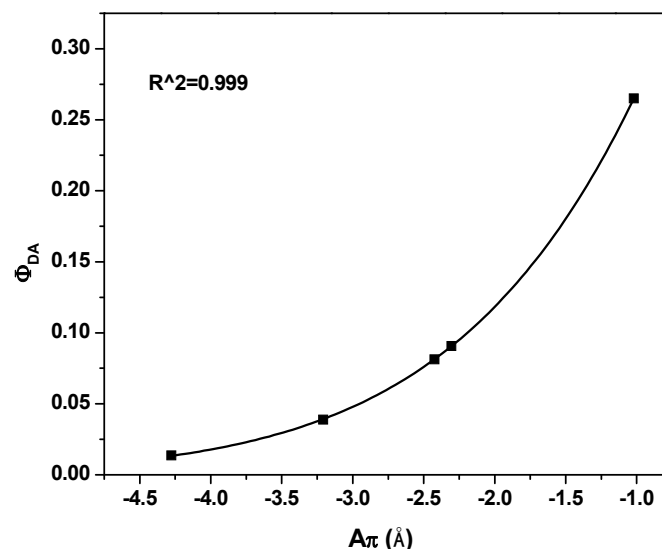


Figure 7. Fluorescence quantum yield versus the conjugated length for PFO/MEH-PPV with various ratios of STNCs.

3.3. Lifetime Decay

The fluorescence lifetime (in Table 1) is differed from the lifetime decay that estimated in this section. The fluorescence lifetime includes the radiative and nonradiative emission, while the lifetime decay contains the radiative emission [24]. Both fluorescence lifetime and lifetime decay demonstrated more information about the influence the STNCs content on the interaction between PFO and MEH-PPV in the excited state.

The lifetime decays obtained at 440 nm and 580 nm for the hybrid thin films with various STNCs content, refer to the emission regions of the donor and acceptor, respectively as shown in Figures 8a–e and 9a–e. A comprehensive investigation including the data collected at 440 and 580 nm was also carried out, confirming the general trends of the data in Table 3. The main fitting parameters χ^2 , B_i and τ_i are presented in Figures 8 and 9 and listed in Table 3 to estimate the effect of STNCs content on the lifetime decay of the hybrid thin film. It can be clearly observed that the donor lifetime (τ_D) increased twice at 5 wt% STNCs content and then continue gradually increased with increment the STNCs. On the other hand, the acceptor lifetime (τ_A) decreased around three times at 5 wt% STNCs content and then continue slight decrease with increment of the STNCs. Increasing donor lifetime proves the increase in conjugation length whereas decreasing the acceptor lifetime proves the enhance in the energy transfer, which are compatible with the previous findings.

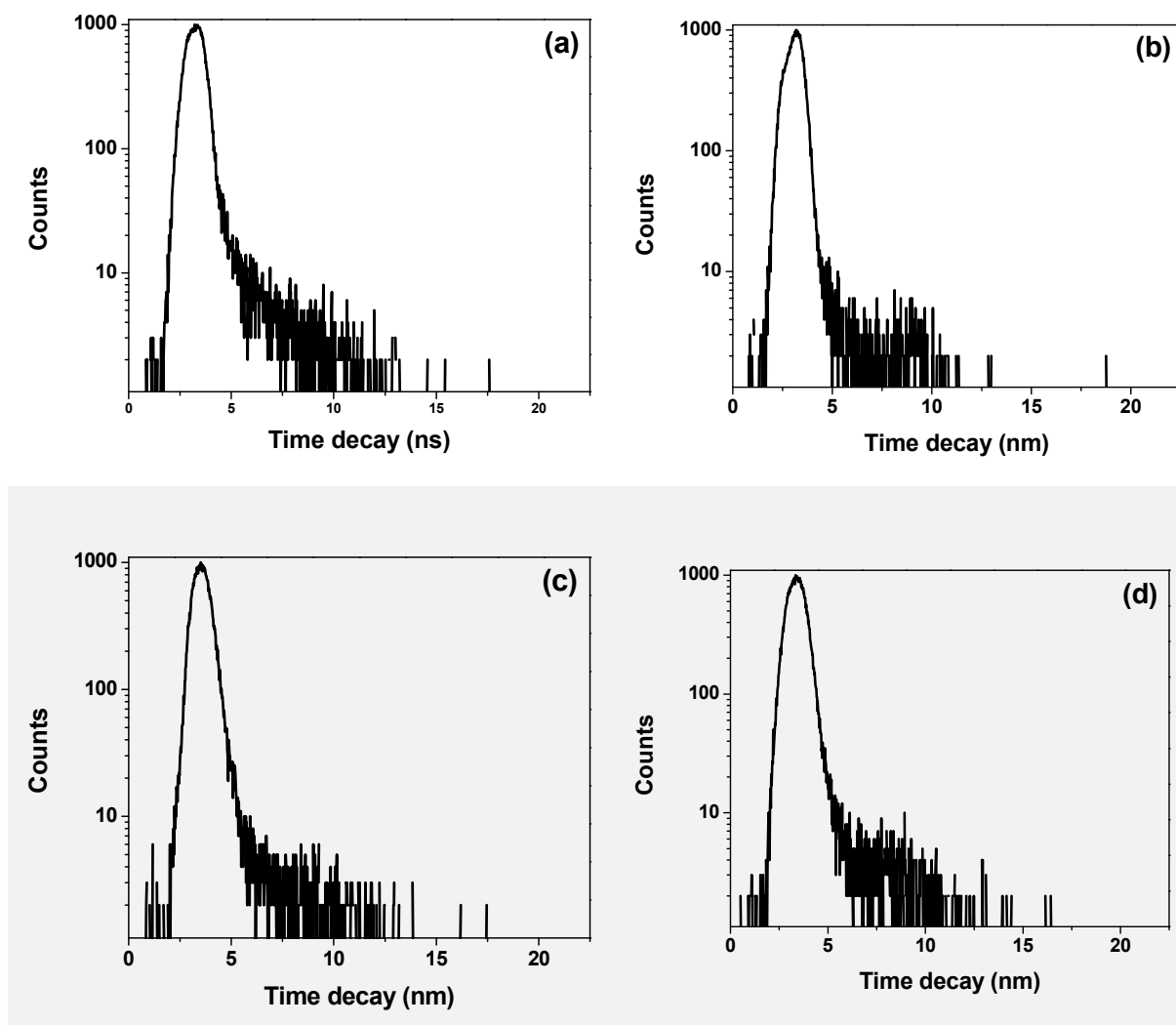


Figure 8. Cont.

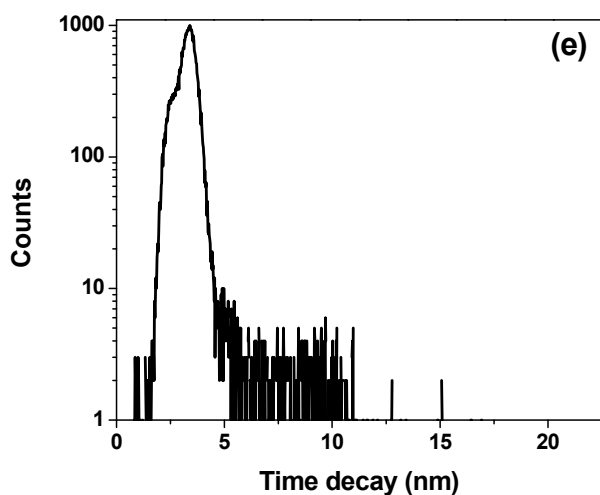


Figure 8. Lifetime decays of PFO/10 wt% MEH-PPV with various ratios of STNCs (a) 0, (b) 5 wt%, (c) 10 wt%, (d) 15 wt% & (e) 20 wt% at emission wavelength of 440 nm. λ_{ex} = 376.4 nm.

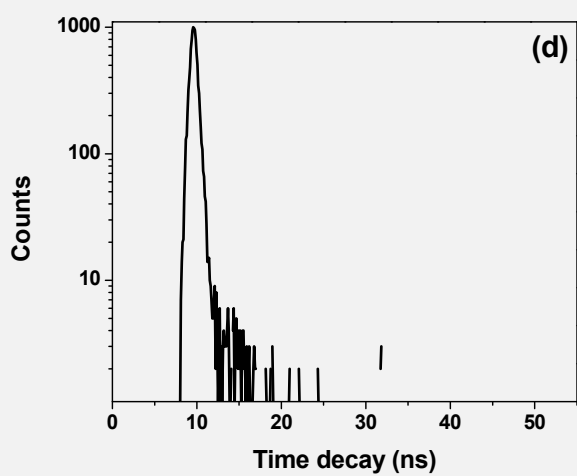
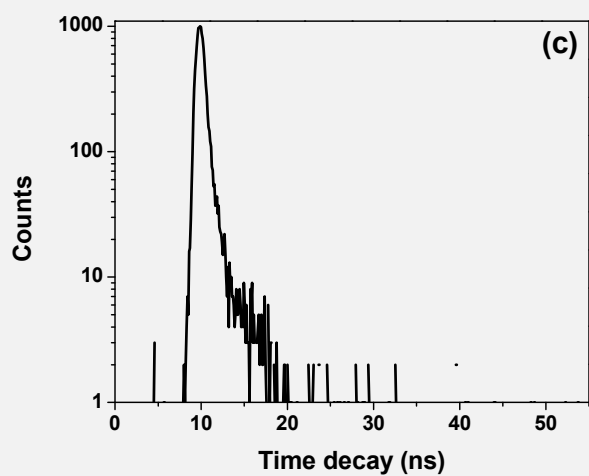
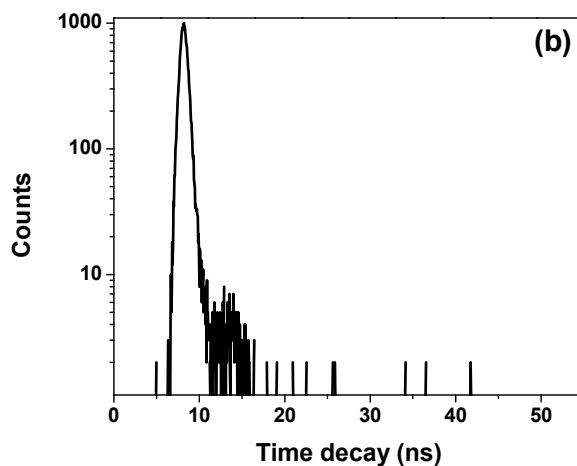
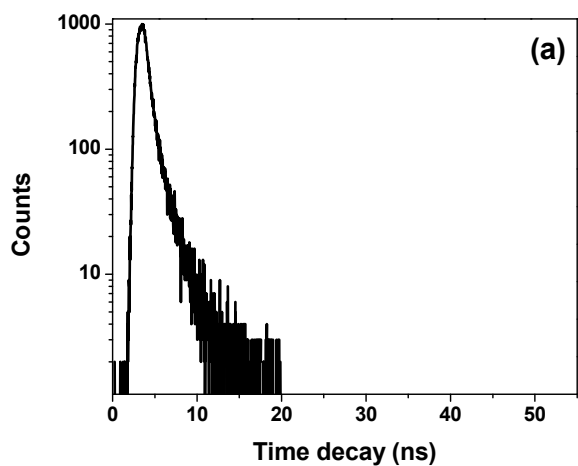


Figure 9. Cont.

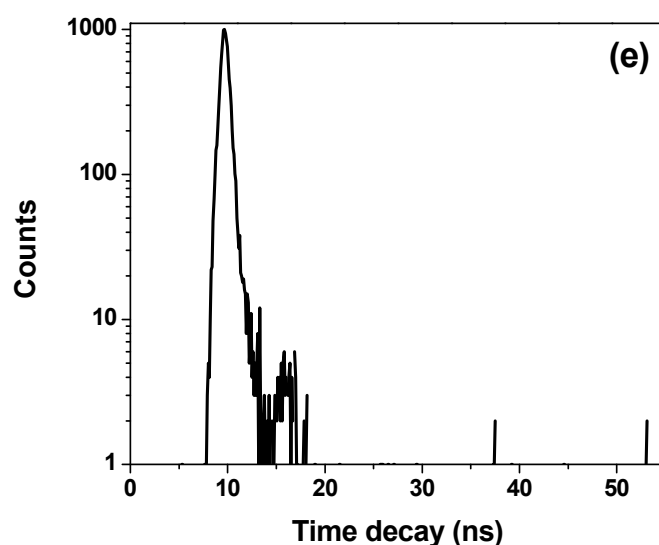


Figure 9. Lifetime decays of PFO/10 wt% MEH-PPV with various ratios of STNCs (a) 0, (b) 5 wt%, (c) 10 wt%, (d) 15 wt% & (e) 20 wt% at emission wavelength of 580 nm. $\lambda_{ex} = 376.4$ nm.

Table 3. Main fitting parameters and lifetime decays of PFO/10 wt% MEH-PPV hybrid thin film with various content of STNCs.

STNCs (wt%)	At λ_{em} . 440 nm				At λ_{em} . 580 nm					
	Relative Amplitude B	Donor Lifetime τ_D (ps)	χ^2	Relative Amplitude		Acceptor Lifetime (ps)				
				B ₁	B ₂	τ_1	τ_2	τ_A (ps)	χ^2	
0	0.316	60	1.784	0.049	0.004	461	1766	772	1.138	
5	0.160	110	1.198	0.160	-	275	-	275	1.069	
10	0.432	116	1.095	0.432	-	234	-	234	1.069	
15	0.574	114	0.912	0.298	-	264	-	264	0.848	
20	0.660	178	0.982	0.555	-	253	-	253	0.908	

4. Conclusions

The modification in the photophysical properties of the donor/acceptor hybrid thin films was achieved by the incorporation of various STNCs content. The significant improved emission intensity of both PFO and MEH-PPV and weak absorption of MEH-PPV in the hybrid thin films refer to enhance energy transfer from PFO to MEH-PPV with an increment of STNCs. The shorter values of ϕ_{DA} and τ_{DA} compared with that of pure PFO thin film indicate the efficient energy transfer from PFO to MEH-PPV with addition of the STNCs. The Förster radius (R_0) was tuned from 43.7 to 75.6 Å where RDA increased from 22.6 to 69.0 Å when the STNCs content increased from 0 to 20 wt%. The critical concentration varied from 5.4 to 1.0 mM while the conjugation length slightly increased from -4.278 to -1.020 Å with the increment of the STNCs from 0 to 20 wt%. Therefore, such donor/acceptor/STNCs composite is believed to be unique potential for designing new materials for optoelectronic devices.

Author Contributions: Conceptualization, B.A.A.-A.; methodology, B.A.A.-A. and H.M.G.; validation, B.A.A.-A., M.H.H.J., M.S.A., S.M.H.Q., A.F and W.M.M.; formal analysis, B.A.A.-A.; investigation, B.A.A.-A. and S.M.H.Q.; data curation, B.A.A.-A. and W.M.M.; writing—original draft preparation, B.A.A.-A.; writing—review and editing, B.A.A.-A. and A.F; visualization, B.A.A.-A. and M.H.H.J.; supervision, B.A.A.-A.; project administration, B.A.A.-A.; funding acquisition, B.A.A.-A. and M.S.A. All authors have read and agreed to the published version of the manuscript.

Funding: This research received no external funding.

Institutional Review Board Statement: Not applicable.

Informed Consent Statement: Not applicable.

Data Availability Statement: The data presented in this study are available on request from the corresponding author.

Acknowledgments: This Project was funded by the National Plan for Science, Technology and Innovation (MAARIFAH), King Abdulaziz City for Science and Technology, Kingdom of Saudi Arabia, Award Number (2-17-01-001-0037).

Conflicts of Interest: The authors declare no conflict of interest.

References

1. Al-Asbahi, B.A.; Jumali, M.H.H.; Yap, C.C.; Flaifel, M.H.; Salleh, M.M. Photophysical properties and energy transfer mechanism of PFO/Fluorol 7GA hybrid thin films. *J. Lumin.* **2013**, *142*, 57–65. [[CrossRef](#)]
2. Al-Asbahi, B.A.; Jumali, M.H.H.; AlSalhi, M.S. Enhanced Optoelectronic Properties of PFO/Fluorol 7GA Hybrid Light Emitting Diodes via Additions of TiO₂ Nanoparticles. *Polymers* **2016**, *8*, 334. [[CrossRef](#)] [[PubMed](#)]
3. Chen, C.-T. Evolution of Red Organic Light-Emitting Diodes: Materials and Devices. *Chem. Mater.* **2004**, *16*, 4389–4400. [[CrossRef](#)]
4. Buckley, A.; Rahn, M.; Hill, J.; Cabanillas-Gonzalez, J.; Fox, A.; Bradley, D. Energy transfer dynamics in polyfluorene-based polymer blends. *Chem. Phys. Lett.* **2001**, *339*, 331–336. [[CrossRef](#)]
5. Al-Asbahi, B.A.; Alsalhi, M.S.; Al-Dwayyan, A.S.; Jumali, M.H. Förster-type energy transfer mechanism in PF2/6 to MEH-PPV conjugated polymers. *J. Lumin.* **2012**, *132*, 386–390. [[CrossRef](#)]
6. Wang, R.; Shi, Z.; Zhang, C.; Zhang, A.; Chen, J.; Guo, W.; Sun, Z. Facile synthesis and controllable bromination of asymmetrical intermediates of perylene monoanhydride/monoimide diester. *Dyes Pigment.* **2013**, *98*, 450–458. [[CrossRef](#)]
7. Al-Asbahi, B.A.; Qaid, S.M.; Jumali, M.H.; AlSalhi, M.S.; Aldwayyan, A.S. Long-range dipole–dipole energy transfer enhancement via addition of SiO₂/TiO₂ nanocomposite in PFO/MEH-PPV hybrid thin films. *J. Appl. Polym. Sci.* **2019**, *136*, 47845. [[CrossRef](#)]
8. Bhattacharyya, S.; Sen, T.; Patra, A. Host–guest energy transfer: Semiconducting polymer nanoparticles and au nanoparticles. *J. Phys. Chem. C* **2010**, *114*, 11787–11795. [[CrossRef](#)]
9. Al-Asbahi, B.A. Influence of SiO₂/TiO₂ nanocomposite on the optoelectronic properties of PFO/MEH-PPV-based OLED devices. *Polymers* **2018**, *10*, 800. [[CrossRef](#)]
10. Al-Asbahi, B.A.; Qaid, S.M.; Ghaithan, H.M.; Farooq, W. Enhancing the Optical and Optoelectronic Properties of MEH-PPV-Based Light-Emitting Diodes by Adding SiO₂/TiO₂ Nanocomposites. *J. Noncryst. Solids* **2020**, *552*, 120429. [[CrossRef](#)]
11. Catauro, M.; Papale, F.; Piccirillo, G.; Bollino, F. PEG-based organic–inorganic hybrid coatings prepared by the sol–gel dip-coating process for biomedical applications. *Polym. Eng. Sci.* **2017**, *57*, 478–484. [[CrossRef](#)]
12. Adnan, M.M.; Dalod, A.R.M.; Balci, M.H.; Glaum, J.; Einarsrud, M.-A. In Situ Synthesis of Hybrid Inorganic–Polymer Nanocomposites. *Polymers* **2018**, *10*, 1129. [[CrossRef](#)]
13. Chen, Y.; Wang, Z.; He, Y.; Yoon, Y.J.; Jung, J.; Zhang, G.; Lin, Z. Light-enabled reversible self-assembly and tunable optical properties of stable hairy nanoparticles. *Proc. Natl. Acad. Sci. USA* **2018**, *115*, E1391–E1400. [[CrossRef](#)]
14. Al-Asbahi, B.A. Influence of anatase titania nanoparticles content on optical and structural properties of amorphous silica. *Mater. Res. Bull.* **2017**, *89*, 286–291. [[CrossRef](#)]
15. Jumali, M.H.H.; Al-Asbahi, B.A.; Yap, C.C.; Salleh, M.M.; Alsalhi, M.S. Optical properties of poly (9,9'-di-n-octylfluorenyl-2,7-diyl)/amorphous SiO₂ nanocomposite thin films. *Sains Malays.* **2013**, *42*, 1151–1157.
16. Ginger, D.; Greenham, N. Charge separation in conjugated-polymer/nanocrystal blends. *Synth. Met.* **1999**, *101*, 425–428. [[CrossRef](#)]
17. Yang, S.; Nguyen, T.; Le Rendu, P.; Hsu, C. Optical and electrical properties of PPV/SiO₂ and PPV/TiO₂ composite materials. *Compos. Part A Appl. Sci. Manuf.* **2005**, *36*, 509–513. [[CrossRef](#)]
18. Zou, J.; Le Rendu, P.; Musa, I.; Yang, S.; Dan, Y.; Ton-That, C.; Nguyen, T. Investigation of the optical properties of polyfluorene/ZnO nanocomposites. *Thin Solid Films* **2011**, *519*, 3997–4003. [[CrossRef](#)]
19. Park, D.H.; Kim, M.S.; Joo, J. Hybrid nanostructures using π -conjugated polymers and nanoscale metals: Synthesis, characteristics, and optoelectronic applications. *Chem. Soc. Rev.* **2010**, *39*, 2439–2452. [[CrossRef](#)] [[PubMed](#)]
20. Jumali, M.H.H.; Al-Asbahi, B.A.; Yap, C.C.; Salleh, M.M.; Alsalhi, M.S. Optoelectronic property enhancement of conjugated polymer in poly (9,9'-di-n-octylfluorenyl-2,7-diyl)/titania nanocomposites. *Thin Solid Films* **2012**, *524*, 257–262. [[CrossRef](#)]
21. Geng, H.; Wang, M.; Han, S.; Peng, R. Enhanced performance of hybrid photovoltaic devices via surface-modifying metal oxides with conjugated polymer. *Sol. Energy Mater. Sol. Cells* **2010**, *94*, 547–553. [[CrossRef](#)]
22. Lakowicz, J.R. *Principles of Fluorescence Spectroscopy*; Springer Science & Business Media: Berlin/Heidelberg, Germany, 2013.
23. Turro, N.J. *Modern Molecular Photochemistry*; University Science Books: Sausalito, CA, USA, 1991.
24. Albani, J. *Structure and Dynamics of Macromolecules: Absorption and Fluorescence Studies*; Elsevier: Amsterdam, The Netherlands, 2004.
25. Schwartz, B.J. Conjugated polymers as molecular materials: How chain conformation and film morphology influence energy transfer and interchain interactions. *Annu. Rev. Phys. Chem.* **2003**, *54*, 141–172. [[CrossRef](#)] [[PubMed](#)]
26. Wu, P.; Brand, L. Resonance Energy Transfer: Methods and Applications. *Anal. Biochem.* **1994**, *218*, 1–13. [[CrossRef](#)] [[PubMed](#)]

-
27. Silfvast, W.T. *Laser Fundamentals*; Cambridge University Press: Cambridge, UK, 2004.
 28. Seth, D.; Chakrabarty, D.; Chakraborty, A.; Sarkar, N. Study of energy transfer from 7-amino coumarin donors to rhodamine 6G acceptor in non-aqueous reverse micelles. *Chem. Phys. Lett.* **2005**, *401*, 546–552. [[CrossRef](#)]
 29. Yamaguchi, Y.; Matsubara, Y.; Ochi, T.; Wakamiya, T.; Yoshida, Z.-I. How the π Conjugation Length Affects the Fluorescence Emission Efficiency. *J. Am. Chem. Soc.* **2008**, *130*, 13867–13869. [[CrossRef](#)]